JNS

LABORATORY INVESTIGATION

Time-dependent and site-dependent morphological changes in rupture-prone arteries: ovariectomized rat intracranial aneurysm model

Tadashi Yamaguchi, MD, Takeshi Miyamoto, MD, PhD, Keiko T. Kitazato, BS, Eiji Shikata, MD, Izumi Yamaguchi, MD, Masaaki Korai, MD, PhD, Kenji Shimada, MD, PhD, Kenji Yagi, MD, PhD, Yoshiteru Tada, MD, PhD, Yoshihito Matsuzaki, BS, Yasuhisa Kanematsu, MD, PhD, and Yasushi Takagi, MD, PhD

Department of Neurosurgery, Graduate School of Biomedical Sciences, Tokushima University, Tokushima, Japan

OBJECTIVE The pathogenesis of intracranial aneurysm rupture remains unclear. Because it is difficult to study the time course of human aneurysms and most unruptured aneurysms are stable, animal models are used to investigate the characteristics of intracranial aneurysms. The authors have newly established a rat intracranial aneurysm rupture model that features site-specific ruptured and unruptured aneurysms. In the present study the authors examined the time course of changes in the vascular morphology to clarify the mechanisms leading to rupture.

METHODS Ten-week-old female Sprague-Dawley rats were subjected to hemodynamic changes, hypertension, and ovariectomy. Morphological changes in rupture-prone intracranial arteries were examined under a scanning electron microscope and the association with vascular degradation molecules was investigated.

RESULTS At 2–6 weeks after aneurysm induction, morphological changes and rupture were mainly observed at the posterior cerebral artery; at 7–12 weeks they were seen at the anterior Willis circle including the anterior communicating artery. No aneurysms at the anterior cerebral artery–olfactory artery bifurcation ruptured, suggesting that the inception of morphological changes is site dependent. On week 6, the messenger RNA level of matrix metalloproteinase–9, interleukin-1β, and the ratio of matrix metalloproteinase–9 to the tissue inhibitor of metalloproteinase–2 was significantly higher at the posterior cerebral artery, but not at the anterior communicating artery, of rats with aneurysms than in sham-operated rats. These findings suggest that aneurysm rupture is attributable to significant morphological changes and an increase in degradation molecules.

CONCLUSIONS Time-dependent and site-dependent morphological changes and the level of degradation molecules may be indicative of the vulnerability of aneurysms to rupture.

https://thejns.org/doi/abs/10.3171/2019.6.JNS19777

KEYWORDS animal models; intracranial aneurysm; subarachnoid hemorrhage; morphology; degradation molecules; vascular disorders

Surgery to prevent subarachnoid hemorrhage (SAH) may elicit complications. Hence, new approaches including pharmacological treatments are required. Based on epidemiological data that the incidence of intracranial aneurysm formation and rupture is higher in women—especially postmenopausal women—than in men,[9,11] we first developed an aneurysm model in female rats subjected to ovariectomy (OVX). In these rats, the rate of morphological changes and aneurysm formation at the anterior cerebral artery–olfactory artery (ACA-OlfA) bifurcation was much higher than in non-OVX and male rats.[13,14,19,27,28,31] We also demonstrated the efficacy of drugs with antihypertensive, antiinflammatory, and antioxidative effects and suggested the possibility of pharmacological prevention of aneurysm formation and growth.[17,27,28,31]

In a prospective study, intracranial aneurysm growth was associated with rupture.[16] In another,[5] most of the growing aneurysms did not rupture. According to Sato

ABBREVIATIONS ACA-OlfA = anterior cerebral artery–olfactory artery; ACoA = anterior communicating artery; GAPDH = glyceraldehyde-3-phosphate dehydrogenase; IL-1β = interleukin-1β; MMP-9 = matrix metalloproteinase–9; mRNA = messenger RNA; OVX = ovariectomy; PCA = posterior cerebral artery; qRT-PCR = quantitative reverse transcription polymerase chain reaction; SAH = subarachnoid hemorrhage; SEM = scanning electron microscope; TIMP2 = tissue inhibitor of metalloproteinase–2.

SUBMITTED March 20, 2019. **ACCEPTED** June 11, 2019.
INCLUDE WHEN CITING Published online September 13, 2019; DOI: 10.3171/2019.6.JNS19777.

and Yoshimoto[23] and Sonobe et al.,[26] some aneurysms ruptured shortly after their formation or without exhibiting morphological changes during the follow-up period. Therefore, to identify therapeutic means of preventing aneurysm growth and rupture, the mechanisms triggering aneurysms and their progress to rupture need to be better understood.

To increase the rupture rate by a surgical procedure without using drugs, we established a new intracranial aneurysm model by modifying the hemodynamics in our rat model.[20] We noted an increase in the growth and rupture of aneurysms at the anterior communicating artery (ACoA) and the proximal portion of the posterior cerebral artery (PCA). Approximately 50% of aneurysms at the anterior Willis circle including the ACoA and PCA ruptured within 12 weeks after the surgical procedure. On the other hand, we observed no ruptured aneurysms at the ACA-OlfA bifurcation despite their high incidence (80%–90%) at 12 weeks postinduction. At the rupture-prone PCA, the messenger RNA (mRNA) level of matrix metalloproteinase–9 (MMP-9) was higher, the mRNA level of the tissue inhibitor of metalloproteinase–2 (TIMP2) was lower, and the disequilibrium of MMP-9/TIMP2 was higher than at the ACA-OlfA bifurcation. These findings suggest a relationship between aneurysm rupture and an increase in degradation molecules.

To elucidate the process underlying the progression to rupture, we used our new intracranial rat aneurysm model and compared the time- and site-dependent morphological changes in the wall of aneurysms prone to rupture with the status of the unruptured aneurysm wall. We also examined the mRNA level of vascular degradation–related molecules at the early phase after aneurysm induction.

Methods

Animal Preparation

All animal experiments were approved by the ethics committee of the Institute of Tokushima University Graduate School and conducted in accordance with the National Institutes of Health Guidelines for the Care and Use of Laboratory Animals. Before any procedures, the rats were anesthetized by 2%–4% isoflurane inhalation. Forty-two female Sprague-Dawley rats purchased from Charles River Laboratories Japan, Inc., were housed in a temperature- and humidity-controlled room (approximately 23°C and 50%, respectively) under a 12-hour light cycle (8 AM–8 PM) and allowed free access to food and water.

Induction of Intracranial Aneurysms

Intracranial aneurysms were induced as detailed elsewhere.[20] As shown Fig. 1A, 10-week-old female rats (230–260 g) were subjected to ligation of the left common carotid artery and the right external carotid and right pterygopalatine arteries to elicit hemodynamic stress. Immediately after ligation they underwent bilateral OVX. They then received a high-salt diet (8% sodium chloride). Two weeks later, first the right posterior renal artery was ligated to induce hypertension, and then the left posterior renal artery was ligated 2 weeks after that. All rats were anesthetized by 2%–4% isoflurane inhalation and the subcutaneous injection of 0.25% bupivacaine. During 1 week in recovery after renal artery ligation, the rats that underwent operation were fed with a normal diet.

Experimental Design

Of 42 rats subjected to intracranial aneurysm induction, 6 died within the first week due to surgery-related issues; they were excluded from this study. Aneurysm rupture was suspected when the rats died or exhibited abnormal neurological behavior and manifested a significant weight loss (> 30 g/day, approximately 10% of their body weight). The rats were euthanized by 2%–4% isoflurane inhalation. In these rats, we used a stereomicroscope to check for SAH due to the rupture of intracranial aneurysms. The lesions were recorded as aneurysms at the anterior Willis circle when they had arisen at the ACoA, the internal carotid artery, or the middle cerebral artery, and as PCA aneurysms when they were located at the proximal portion of the left PCA. The vascular surface and the structural changes were inspected on corrosion casts at 6 and 12 weeks after aneurysm induction. After 6 weeks of observation (early period, 36 rats), one-third of the rats (n = 12) was randomly chosen by a blinded observer and used for the preparation of vascular corrosion casts to assess structure and morphological changes. After 12 weeks of observation (late period, 20 rats), we also prepared vascular corrosion casts of rats without rupture. Blood pressure measurements were obtained before ligation of the posterior renal artery and at 4-week intervals after aneurysm induction by using the tail-cuff, auto-pickup method (Softron). The study protocol is shown in Fig. 1A.

Vascular Corrosion Casts

Vascular corrosion casts were prepared 6 and 12 weeks after aneurysm induction.[13] The rats were transcardially perfused with heparinized phosphate-buffered saline followed by the injection of Batson's No. 17 plastic (Polysciences Inc.). The left PCA, the ACoA, and the right ACA-OlfA bifurcation were inspected on the casts using a scanning electron microscope (SEM; VE8800; Keyence). Two blinded observers evaluated morphological changes at the endothelial cell imprints of each artery and measured the angle and diameter of the PCA (Fig. 2). With the basilar artery in the horizontal position, the angle at the midpoint of the PCA arch was measured using software provided on the SEM.

RNA Isolation and Real-Time Quantitative Reverse Transcription Polymerase Chain Reaction Assay

The mRNA level in another set of sham-operated and aneurysm model rats (each set contained 8–10 rats) was compared by real-time quantitative reverse transcription polymerase chain reaction (qRT-PCR) assay. Age-matched sham-operated rats and rats subjected to aneurysm induction 6 weeks earlier were euthanized. Before sampling, 2 rats with ruptured aneurysms were excluded because their time of death was not ascertained. Total RNA at the ACoA and the left PCA was isolated and extracted with the MagNA Pure RNA isolation kit (Roche) and the MagNA lyser (Roche). We used Transcriptor Universal cDNA

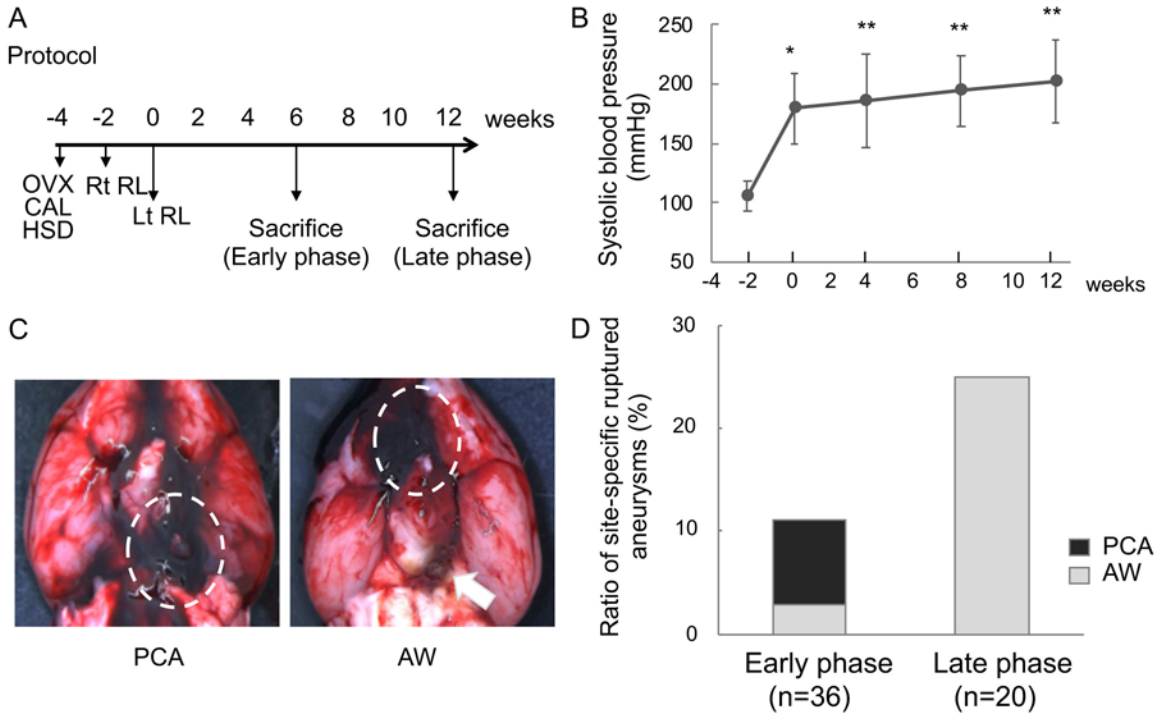

FIG. 1. Time-dependent changes in site-specific aneurysm rupture. **A:** Experimental protocol. CAL = carotid artery ligation; HSD = high-salt diet; Rt/Lt RL = right/left posterior renal artery ligation. **B:** Sequential changes in the systolic blood pressure measured by the tail-cuff method. The point after the posterior renal artery ligation was defined as the start of observation (time 0). Data are expressed as the mean ± SD. *$p < 0.05$, **$p < 0.01$ versus values before renal artery ligation according to ANOVA followed by the Kruskal-Wallis test. **C:** Representative photographs of SAH due to the rupture of aneurysms at the left PCA (left panel, *white circle*) and the anterior Willis circle (AW) (right panel, *white circle*) including the ACoA, the internal carotid artery, and the middle cerebral artery. This rat first manifested rupture of the PCA aneurysm (right panel, *white arrow*) followed by rupture of the anterior Willis circle aneurysm. **D:** The rate of ruptured PCA aneurysms increased in the early phase (2–6 weeks after aneurysm induction). The incidence of rupture of anterior Willis circle aneurysms rose in the late phase (7–12 weeks postinduction).

Master (Roche) for the reverse transcription of total RNA to cDNA and a LightCycler 2.0 (Roche Diagnostics) for real-time qRT-PCR. The level of MMP-9, TIMP2, interleukin-1β (IL-1β), and glyceraldehyde-3-phosphate dehydrogenase (GAPDH) was recorded. The primers were as follows: for MMP-9, forward 5′-CCT GGA ACT CAC ACA ACG-3′, reverse 5′-GAG GTC ATA GGT CAC GTA GG-3′; for TIMP2, forward 5′-CCC TCT GTG ACT TTA TTG TGC-3′, reverse 5′-TGA TGC TCT CTG TGA CC-3′; for IL-1β, forward 5′-TGC AGG CTT CGA GAT GAA C-3′, reverse 5′-AGC TCA TGG AGA ATA CCA CTT G-3′; and for GAPDH, forward 5′-TAC ACT GAG GAC CAG GTT G-3′, reverse 5′-CCC TGT TGC TGT AGC CAT A-3′. The PCR conditions were 95°C for 10 minutes followed by 40 cycles at 95°C for 10 seconds, 60°C for 10 seconds, and 72°C for 8 seconds. We subjected 8–10 samples in each group to real-time qRT-PCR assay to determine the gene expression level. The results were normalized to the expression of GAPDH mRNA.

Statistical Analysis

Statistical analyses were performed using GraphPad Prism version 7.0 software. Sequentially obtained data were analyzed with 1-way ANOVA followed by the Kruskal-Wallis test for multiple group comparisons of the mRNA level and systolic blood pressure. Fisher's exact test was used to analyze the morphological stages. Data on the arterial angle and diameter were analyzed with the Student t-test. Data are expressed as the mean ± SD. Differences were considered significant at $p < 0.05$.

Results

Aneurysms at the PCA and the Anterior Willis Circle Ruptured in the Early and Late Phase, Respectively

Elsewhere[20] we reported the site-specific formation of ruptured and unruptured aneurysms in our rat aneurysm model without addressing the time course of morphological changes at each site. In the current study, the systolic blood pressure of the rats was not different from earlier findings.[15] It was increased significantly ($p < 0.05$) 2 weeks after ligation of the unilateral posterior renal artery, and the increase persisted throughout the 12-week observation period (Fig. 1B).

Aneurysms at the PCA and the anterior Willis circle tended to rupture in the early and late phase, respectively (Fig. 1C); 3 of 36 PCA aneurysms ruptured in the early phase (2–6 weeks postinduction), whereas 5 of 20 aneurysms at the anterior Willis circle ruptured in the late phase (7–12 weeks) (Fig. 1D).

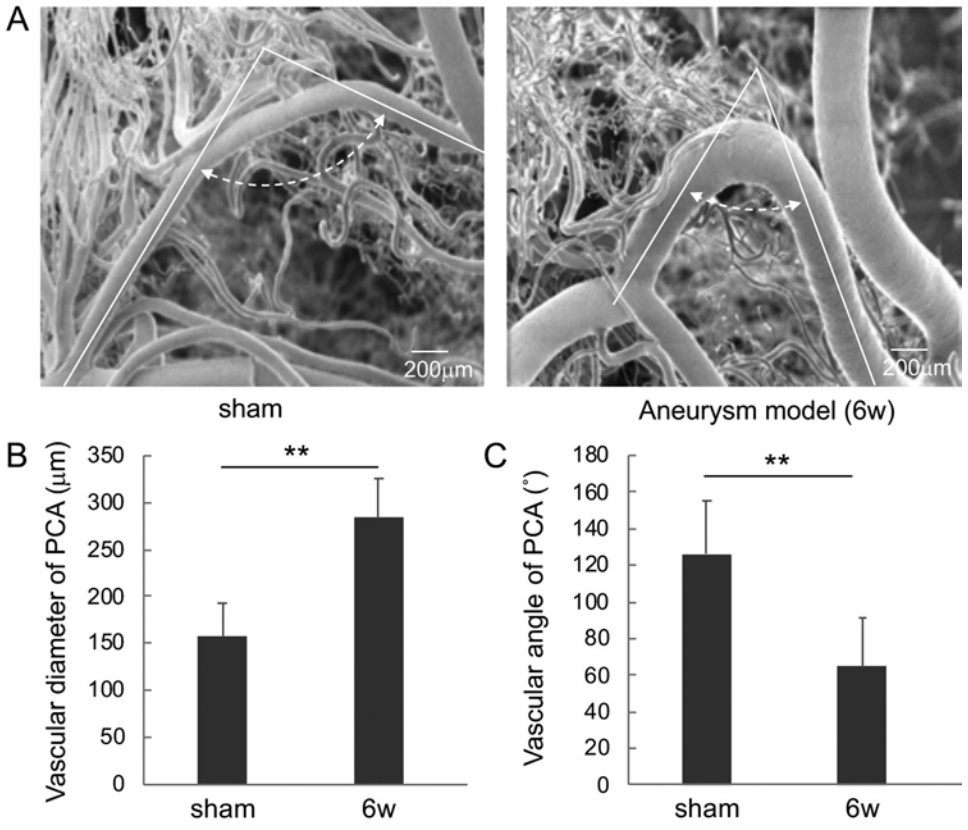

FIG. 2. Changes in the PCA diameter and angle reflecting atypical structural changes in the early phase after aneurysm induction. **A:** Representative images of an age-matched sham-operated rat (*left*) and a rat with aneurysm showing the PCA 6 weeks after aneurysm induction (*right*). **B:** Changes in the diameter of the PCA 6 weeks after aneurysm induction. **C:** Changes in the angle of the PCA on corrosion casts. Measurements were made with software provided on the SEM. Data are expressed as the mean ± SD. **p < 0.01 versus sham-operated rats by Student t-test.

Rapid Changes in the Structure of PCA Aneurysms Led to Rupture

To better understand the early-phase rupture of PCA aneurysms, we recorded the time course of changes in the PCA diameter and angle. In age-matched sham-operated rats, the proximal portion of the PCA was arcuate without bifurcation up to its connection to the posterior communicating artery (Fig. 2A).

At 6 weeks, the PCA diameter was significantly larger in rats with aneurysms than in the sham-operated animals and the PCA angle was much sharper (Fig. 2B and C). There was no significant difference in these metrics at 6 and 12 weeks after aneurysm induction (data not shown).

Morphological Changes Appeared Early at the PCA and Gradually at the ACoA

At 6 and 12 weeks after aneurysm induction, morphological changes observed on corrosion casts were classified into 3 stages: stage 0, normal with regular endothelial cell imprints; stage 1, rough, irregular endothelial cells; and stage 2, aneurysmal changes including an increase in the diameter of the parent artery and collapse of endothelial cell imprints (Fig. 3).

Six weeks after aneurysm induction, the wall of the PCA exhibited slight to moderate morphological changes (stage 1 or 2) in all rats. We did not observe advanced aneurysmal changes at the PCA (Fig. 4A), suggesting that PCA aneurysms ruptured immediately after the inception of morphological changes. The incidence of such changes at the ACoA was significantly higher at 12 than at 6 weeks (75.6% vs 33.3%, $p = 0.045$) and was occasionally accompanied by aneurysmal changes (Fig. 4B), suggesting that in contrast to PCA aneurysms, ACoA aneurysms grew slowly and persistently. Although morphological changes were observed at 6 and 12 weeks postinduction in 53.8% and 85.7% of ACA-OlfA aneurysms, respectively (Fig. 4C), the lesions did not rupture.

The Imbalance Between Vascular Degradation Molecules and Tissue Inhibitors Was Associated With Rapid Morphological Changes and the Rupture of PCA Aneurysms

Elsewhere[17] we reported changes in the vascular inflammation– and degradation–related molecules MMP-9, IL-1β, and TIMP2 in the cerebral vascular wall prone to rupture 12 weeks after aneurysm induction in ovariectomized rats. To examine the level of these molecules 6 weeks after the induction of PCA aneurysms that we found to be prone to rupture, we recorded the mRNA level of MMP-9, IL-1β, and TIMP2 at the PCA and ACoA and

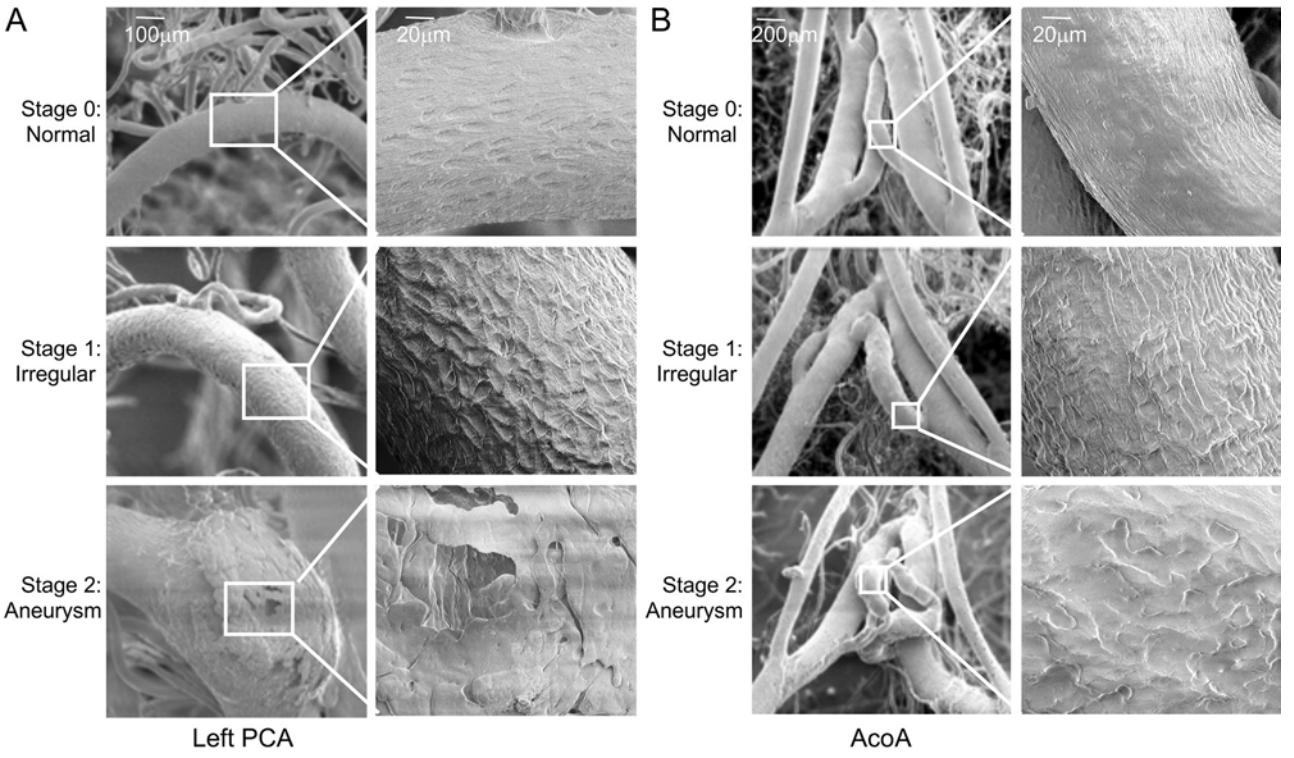

FIG. 3. Representative images and classification of vascular morphological changes on corrosion casts mirrored on SEM images. **A:** Morphological changes in the left PCA. **B:** Morphological changes in the ACoA. Stage 0, normal, regular endothelial cell imprints; stage 1, rough, irregular endothelial cell imprints; and stage 2, aneurysmal changes including an increase in the diameter of the parent artery and collapse of endothelial cell imprints.

compared them with findings in the PCA of age-matched, sham-operated rats. As shown in Fig. 5, the mRNA level of IL-1β and MMP-9 in the PCA of rats harboring aneurysms was significantly higher than in our sham-operated rats ($p < 0.01$ between each rat group). In the ACoA, the mRNA level of IL-1β, but not of MMP-9, was also significantly higher than in the sham-operated rats ($p < 0.05$) (Fig. 5A and B). In the rats with aneurysms, the mRNA level of TIMP2 was significantly higher at the ACoA than at the PCA ($p < 0.01$) (Fig. 5C). There was no difference in the mRNA level of TIMP2 at the PCA of rats with aneurysms and sham-operated rats, suggestive of a compensatory increase in TIMP2 at the ACoA. In rats with aneurysms, the ratio of MMP-9/TIMP2 at the PCA was higher than at the ACoA and significantly higher than in the sham-operated rats ($p < 0.01$, Fig. 5D).

Discussion

Using our new rat intracranial aneurysm model, as far as we know, we are the first to document the time- and site-dependent morphological changes at arteries that are prone and not prone to rupture. We detected morphological and structural PCA changes in the early phase after aneurysm induction. They were accompanied by an imbalance between the mRNA level of vascular degradation and protection molecules. On the other hand, morphological changes at the ACoA proceeded gradually and led to rupture in the late phase. Our findings suggest that aneurysm rupture is attributable to significant changes in the vascular morphology and an increase in vascular inflammation– and degradation–related molecules.

Rapid morphological changes, enlargement of the diameter of the PCA, its sharp angle, and rupture of PCA aneurysms were observed only in the early phase after aneurysm induction. The rapid structural changes may at least partly account for the early-phase rupture of PCA aneurysms. On the other hand, the late-phase rupture of aneurysms at the anterior Willis circle including the ACoA may be associated with the gradual progression of morphological changes. Previously we demonstrated that enlargement of the left PCA diameter was due to an increase in the blood flow volume at the basilar artery 4 weeks after aneurysm induction.[20] Angiographic findings reported by Cai et al.[7] revealed a gradual increase in the diameter of the ACA. The gradual growth of aneurysms at the ACoA and the small size of aneurysms at the ACA-OlfA bifurcation may account in part for their rupture and nonrupture, respectively.[20] Thus, changes in the vascular structure may at least partly contribute to the vulnerability of the vascular wall.

The activation of MMPs through IL-1β promotes extracellular matrix degradation.[10,22] The regulation of these molecules is associated with the preservation of elastin and collagen.[18,29,30] According to Nakagawa et al.,[21] the concentration of soluble human elastin fragments was significantly higher in the lumen of ruptured than unruptured

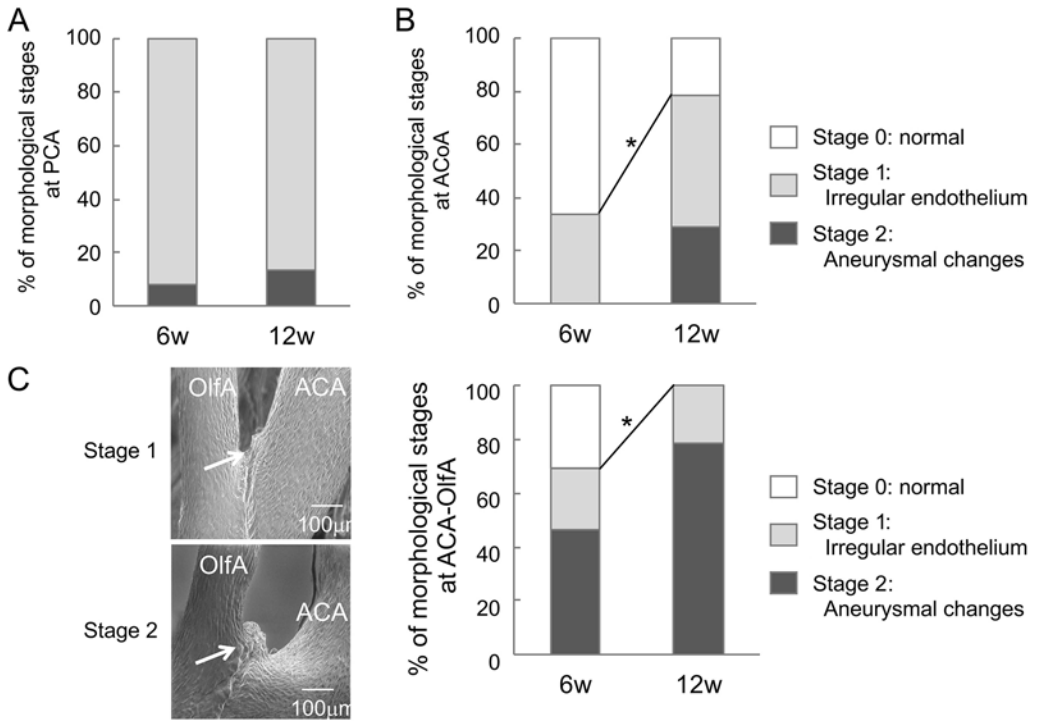

FIG. 4. Morphological changes in the wall of the PCA, ACoA, and ACA-OlfA in the early and late phase after aneurysm induction. **A:** Incidence of morphological changes at PCA mirrored on SEM at 6 and 12 weeks after aneurysm induction. **B:** Morphological changes in the ACoA mirrored on SEM were greater at 12 weeks than at 6 weeks after aneurysm induction. **C:** SEM images of morphological changes at the ACA-OlfA bifurcation (left panel, *white arrows*). The morphological changes were greater at 12 weeks than at 6 weeks after aneurysm induction (right panel). For the staging of morphological changes, see Fig. 3. *$p < 0.05$ by Fisher's exact test.

intracranial aneurysms. Others[1,8] reported that the expression of MMP-9 and IL-1β was related to the formation and rupture of intracranial aneurysms. Our earlier studies[17,20] revealed that the increase in MMP-9 and the imbalance between MMP-9 and TIMP2 in the intracranial vascular wall were associated with rupture in rats that had been ovariectomized 12 weeks earlier. In the current study we observed a significant increase in the MMP-9 and IL-1β level and an imbalance between MMP-9 and TIMP2 at the PCA prone to rupture 6 weeks after aneurysm induction. The imbalance in vascular degradative and protective molecules in the early phase may be at least partly attributable to rapid morphological changes that lead to aneurysm rupture. In the early phase after aneurysm induction, the imbalance between MMP-9 and TIMP2 was greater at the PCA than at the ACoA. At the ACoA we observed a significant increase in IL-1β but not in MMP-9, nor did we find an imbalance between MMP-9 and TIMP2 in the early phase. These differences may explain the observed morphological changes and the subsequent early-phase rupture of PCA aneurysms. Our findings may reflect the different characteristics of PCA and ACoA aneurysms and point to a relationship between the increase in vascular degradation molecules and aneurysm rupture. However, measurements of only the mRNA level do not permit inferences regarding functional changes.

Sho et al.[24] reported that in their rabbit arteriovenous fistula model, high flow and shear stress induced the expression of MMP-2, MMP-9, and TIMP2 in endothelial and smooth-muscle cells. On the other hand, Berard et al.[4] found that hemodynamic forces and high pressure induced an increase in the mRNA level of MMP-9 and a decrease in the mRNA level of TIMP2 in a human saphenous venous graft model. Although our rats were subjected to hemodynamic changes, we did not directly assess the blood flow and pressure in the PCA and ACoA. Therefore, we cannot address whether the increased mRNA level of MMP-9 and the decreased mRNA level of TIMP2 at the PCA—but not at the ACoA—in the early phase after aneurysm induction are associated with hemodynamic effects.

Human studies revealed that a steep bifurcation angle increased the risk for developing intracranial aneurysms.[25,33,34] There was also a significant positive correlation between the diameter of the arterial bifurcation branch and the aneurysm size.[33,34] The maximum dome diameter was significantly greater in ruptured than in unruptured sidewall intracranial aneurysms,[2,3] and geometrical analysis of the parent vessel of 68 aneurysms, including 14 sidewall aneurysms, revealed a significant positive correlation between the aneurysm height and the diameter of draining arteries.[12] Computational flow dynamics analysis showed that shear stress and pressure on the vascular wall were higher in sidewall aneurysms in curved than in straight arteries. Also, a localized increase in shear stress, velocity, and pressure were correlated with aneurysm rupture points.[12] These observations led us to suspect that the

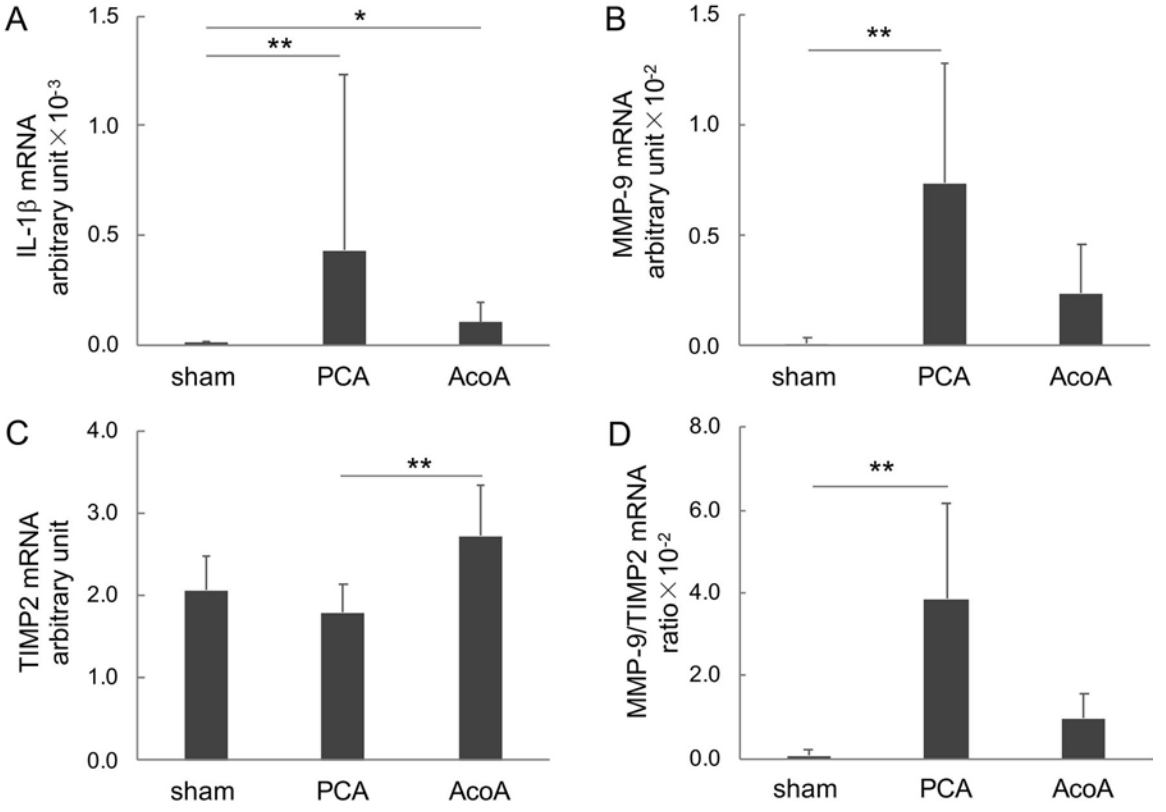

FIG. 5. Changes in vascular inflammation– and degradation–related molecules and their imbalance in the PCA and ACoA 6 weeks after aneurysm induction. The mRNA level of IL-1β (**A**), MMP-9 (**B**), TIMP2 (**C**), and the ratio of MMP-9/TIMP2 (**D**) at the PCA and ACoA 6 weeks after aneurysm induction and at the PCA of age-matched sham-operated rats. The mRNA level was determined by real-time qRT-PCR and normalized by GAPDH. Data are expressed as the mean ± SD (8–10 rats in each group). *$p < 0.05$ and **$p < 0.01$ by ANOVA followed by the Kruskal-Wallis test.

curved structure of the PCA and the expanding aneurysm diameter in our rat model may render these aneurysms similar in type to human intracranial sidewall aneurysms.

Yonekura[32] divided the growth and rupture process of intracranial aneurysms into 4 patterns, in which pattern 1 was rupture shortly after formation; pattern 2 was rupture in the course of slow growth; pattern 3 was slow growth without rupture; and pattern 4 was slow growth up to a certain size and no change thereafter. In a prospective study of 448 small unruptured intracranial aneurysms,[26] none exhibited pattern 1; 7 (1.6%) showed pattern 2; 30 (6.7%) manifested pattern 3; and 411 (91.7%) were of pattern 4. Only 7 of the 448 aneurysms (1.6%) ruptured eventually. We think that the PCA aneurysms in our rat model were of pattern 1 and that the rapidity of morphological changes resulted in their early-phase rupture. Aneurysms at the anterior Willis circle including the ACoA may reflect pattern 2 due to their slow growth and rupture in the late phase. In some respects, the aneurysms at the ACA-OlfA bifurcation may reflect patterns 3 and 4. Our rat aneurysm model revealed site-specific growth processes and different rupture timing. Rapid morphological changes may be indicative of the vulnerability of aneurysms to rupture.

Our study has some limitations. First, we assessed morphological changes no earlier than 6 weeks after aneurysm induction. Second, although we measured the diameter and the angle of the PCA, individual variations in the ACoA and ACA made such measurements difficult.[6] Third, we did not assess the morphological changes sequentially in individual rats because they were killed at different time points and some rats with ruptured aneurysms were excluded from analysis. Therefore, we cannot rule out sampling bias in the assessment of both morphological changes and the mRNA level of vascular degradation molecules.

Conclusions

Our rat model in which intracranial aneurysms were induced by eliciting hemodynamics changes yielded new evidence that aneurysm rupture was time and site dependent. Structural and morphological changes even in the early phase were accompanied by an increase in vascular degradation molecules. Rapid morphological changes and the increase in vascular degradation molecules may be indicative of the vulnerability of aneurysms to rupture.

References

1. Aoki T, Kataoka H, Morimoto M, Nozaki K, Hashimoto N: Macrophage-derived matrix metalloproteinase-2 and -9 promote the progression of cerebral aneurysms in rats. **Stroke 38:**162–169, 2007
2. Baharoglu MI, Lauric A, Gao BL, Malek AM: Identification

of a dichotomy in morphological predictors of rupture status between sidewall- and bifurcation-type intracranial aneurysms. **J Neurosurg 116:**871–881, 2012
3. Baharoglu MI, Schirmer CM, Hoit DA, Gao BL, Malek AM: Aneurysm inflow-angle as a discriminant for rupture in sidewall cerebral aneurysms: morphometric and computational fluid dynamic analysis. **Stroke 41:**1423–1430, 2010
4. Berard X, Déglise S, Alonso F, Saucy F, Meda P, Bordenave L, et al: Role of hemodynamic forces in the ex vivo arterialization of human saphenous veins. **J Vasc Surg 57:**1371–1382, 2013
5. Bor AS, Tiel Groenestege AT, terBrugge KG, Agid R, Velthuis BK, Rinkel GJ, et al: Clinical, radiological, and flow-related risk factors for growth of untreated, unruptured intracranial aneurysms. **Stroke 46:**42–48, 2015
6. Brown JO: The morphology of circulus arteriosus cerebri in rats. **Anat Rec 156:**99–106, 1966
7. Cai J, He C, Yuan F, Chen L, Ling F: A novel haemodynamic cerebral aneurysm model of rats with normal blood pressure. **J Clin Neurosci 19:**135–138, 2012
8. Chalouhi N, Ali MS, Jabbour PM, Tjoumakaris SI, Gonzalez LF, Rosenwasser RH, et al: Biology of intracranial aneurysms: role of inflammation. **J Cereb Blood Flow Metab 32:**1659–1676, 2012
9. de Rooij NK, Linn FH, van der Plas JA, Algra A, Rinkel GJ: Incidence of subarachnoid haemorrhage: a systematic review with emphasis on region, age, gender and time trends. **J Neurol Neurosurg Psychiatry 78:**1365–1372, 2007
10. Eberhardt W, Huwiler A, Beck KF, Walpen S, Pfeilschifter J: Amplification of IL-1β-induced matrix metalloproteinase-9 expression by superoxide in rat glomerular mesangial cells is mediated by increased activities of NF-κB and activating protein-1 and involves activation of the mitogen-activated protein kinase pathways. **J Immunol 165:**5788–5797, 2000
11. Harrod CG, Batjer HH, Bendok BR: Deficiencies in estrogen-mediated regulation of cerebrovascular homeostasis may contribute to an increased risk of cerebral aneurysm pathogenesis and rupture in menopausal and postmenopausal women. **Med Hypotheses 66:**736–756, 2006
12. Hassan T, Timofeev EV, Saito T, Shimizu H, Ezura M, Matsumoto Y, et al: A proposed parent vessel geometry-based categorization of saccular intracranial aneurysms: computational flow dynamics analysis of the risk factors for lesion rupture. **J Neurosurg 103:**662–680, 2005
13. Jamous MA, Nagahiro S, Kitazato KT, Satoh K, Satomi J: Vascular corrosion casts mirroring early morphological changes that lead to the formation of saccular cerebral aneurysm: an experimental study in rats. **J Neurosurg 102:**532–535, 2005
14. Jamous MA, Nagahiro S, Kitazato KT, Satomi J, Satoh K: Role of estrogen deficiency in the formation and progression of cerebral aneurysms. Part I: experimental study of the effect of oophorectomy in rats. **J Neurosurg 103:**1046–1051, 2005
15. Jamous MA, Nagahiro S, Kitazato KT, Tamura T, Kuwayama K, Satoh K: Role of estrogen deficiency in the formation and progression of cerebral aneurysms. Part II: experimental study of the effects of hormone replacement therapy in rats. **J Neurosurg 103:**1052–1057, 2005
16. Juvela S: Growth and rupture of unruptured intracranial aneurysms. **J Neurosurg 131:**843–851, 2019
17. Korai M, Kitazato KT, Tada Y, Miyamoto T, Shimada K, Matsushita N, et al: Hyperhomocysteinemia induced by excessive methionine intake promotes rupture of cerebral aneurysms in ovariectomized rats. **J Neuroinflammation 13:**165, 2016
18. Kurzepa J, Kurzepa J, Golab P, Czerska S, Bielewicz J: The significance of matrix metalloproteinase (MMP)-2 and MMP-9 in the ischemic stroke. **Int J Neurosci 124:**707–716, 2014
19. Matsushita N, Kitazato KT, Tada Y, Sumiyoshi M, Shimada K, Yagi K, et al: Increase in body Na^+/water ratio is associated with cerebral aneurysm formation in oophorectomized rats. **Hypertension 60:**1309–1315, 2012
20. Miyamoto T, Kung DK, Kitazato KT, Yagi K, Shimada K, Tada Y, et al: Site-specific elevation of interleukin-1β and matrix metalloproteinase-9 in the Willis circle by hemodynamic changes is associated with rupture in a novel rat cerebral aneurysm model. **J Cereb Blood Flow Metab 37:**2795–2805, 2017
21. Nakagawa D, Zanaty M, Hudson J, Teferi N, Ishii D, Allan L, et al: Plasma soluble human elastin fragments as an intraaneurysmal localized biomarker for ruptured intracranial aneurysm. **J Am Heart Assoc 7:**e010051, 2018
22. Poljak M, Lim R, Barker G, Lappas M: Class I to III histone deacetylases differentially regulate inflammation-induced matrix metalloproteinase 9 expression in primary amnion cells. **Reprod Sci 21:**804–813, 2014
23. Sato K, Yoshimoto Y: Risk profile of intracranial aneurysms: rupture rate is not constant after formation. **Stroke 42:**3376–3381, 2011
24. Sho E, Sho M, Singh TM, Nanjo H, Komatsu M, Xu C, et al: Arterial enlargement in response to high flow requires early expression of matrix metalloproteinases to degrade extracellular matrix. **Exp Mol Pathol 73:**142–153, 2002
25. Song J, Zhu F, Qian Y, Ou C, Cai J, Zou X, et al: Morphological and hemodynamic differences between aneurysmal middle cerebral artery bifurcation and contralateral nonaneurysmal anatomy. **Neurosurgery 81:**779–786, 2017
26. Sonobe M, Yamazaki T, Yonekura M, Kikuchi H: Small unruptured intracranial aneurysm verification study: SUAVe study, Japan. **Stroke 41:**1969–1977, 2010
27. Tada Y, Yagi K, Kitazato KT, Tamura T, Kinouchi T, Shimada K, et al: Reduction of endothelial tight junction proteins is related to cerebral aneurysm formation in rats. **J Hypertens 28:**1883–1891, 2010
28. Tamura T, Jamous MA, Kitazato KT, Yagi K, Tada Y, Uno M, et al: Endothelial damage due to impaired nitric oxide bioavailability triggers cerebral aneurysm formation in female rats. **J Hypertens 27:**1284–1292, 2009
29. Tummers AM, Mountain DJ, Mix JW, Kirkpatrick SS, Cassada DC, Stevens SL, et al: Serum levels of matrix metalloproteinase-2 as a marker of intimal hyperplasia. **J Surg Res 160:**9–13, 2010
30. Yagi K, Kitazato KT, Uno M, Tada Y, Kinouchi T, Shimada K, et al: Edaravone, a free radical scavenger, inhibits MMP-9-related brain hemorrhage in rats treated with tissue plasminogen activator. **Stroke 40:**626–631, 2009
31. Yagi K, Tada Y, Kitazato KT, Tamura T, Satomi J, Nagahiro S: Ibudilast inhibits cerebral aneurysms by down-regulating inflammation-related molecules in the vascular wall of rats. **Neurosurgery 66:**551–559, 2010
32. Yonekura M: Importance of prospective studies for deciding on a therapeutic guideline for unruptured cerebral aneurysm. **Acta Neurochir Suppl 82:**21–25, 2002
33. Zhang XJ, Gao BL, Hao WL, Wu SS, Zhang DH: Presence of anterior communicating artery aneurysm is associated with age, bifurcation angle, and vessel diameter. **Stroke 49:**341–347, 2018
34. Zhang XJ, Gao BL, Li TX, Hao WL, Wu SS, Zhang DH: Association of basilar bifurcation aneurysms with age, sex, and bifurcation geometry. **Stroke 49:**1371–1376, 2018

Disclosures

The authors report no conflict of interest concerning the materials or methods used in this study or the findings specified in this paper.

Author Contributions

Conception and design: T Yamaguchi, Miyamoto, Kitazato. Acquisition of data: T Yamaguchi, Matsuzaki. Analysis and interpretation of data: T Yamaguchi. Drafting the article: T Yamaguchi. Critically revising the article: Miyamoto, Kitazato, Shikata, I Yamaguchi, Korai, Shimada, Yagi, Tada, Kanematsu, Takagi. Reviewed submitted version of manuscript: T Yamaguchi, Miyamoto, Kitazato. Approved the final version of the manuscript on behalf of all authors: T Yamaguchi. Statistical analysis: T Yamaguchi. Study supervision: T Yamaguchi, Miyamoto, Takagi.

Correspondence

Tadashi Yamaguchi: Graduate School of Biomedical Sciences, Tokushima University, Tokushima, Japan. tadashi117117@hotmail.co.jp.